

## A study of $\text{Li}_2\text{TiOSiO}_4$ and $\text{Li}_2\text{TiOGeO}_4$ by X-ray powder and electron single-crystal diffraction, $^{17}\text{O}$ MAS NMR and O $K$ -edge and Ti $L_{2,3}$ -edge EELS

T. J. BASTOW,<sup>a</sup> G. A. BOTTON,<sup>b</sup> J. ETHERIDGE,<sup>b,c</sup> M. E. SMITH<sup>d</sup> AND H. J. WHITFIELD<sup>c\*</sup>

<sup>a</sup>CSIRO Division of Materials Science and Technology, Private Bag 33, Rosebank MDC, Clayton, Victoria 3169, Australia, <sup>b</sup>Department of Materials Science and Metallurgy, University of Cambridge, Pembroke Street, Cambridge CB2 3QZ, England, <sup>c</sup>Department of Applied Physics, Royal Melbourne Institute of Technology, Box 2476V, Melbourne, Victoria 3001, Australia, and <sup>d</sup>Physics Laboratory, University of Kent, Canterbury, Kent CT2 7NR, England. E-mail: harold.whitfield@rmit.edu.au

(Received 3 February 1998; accepted 15 May 1998)

Dedicated to Professor A. F. Moodie on the occasion of his 75th birthday

### Abstract

X-ray powder and electron single-crystal diffraction of crystals of  $\text{Li}_2\text{TiOSiO}_4$  and  $\text{Li}_2\text{TiOGeO}_4$  showed them to be tetragonal, space group  $P4/nmm$  unit-cell parameters  $a = 6.4379(2)$ ,  $c = 4.40032(2)$  Å for  $\text{Li}_2\text{TiOSiO}_4$  and  $a = 6.6110(8)$ ,  $c = 4.4372(6)$  Å for  $\text{Li}_2\text{TiGeO}_4$ . The compounds are isostructural with their sodium analogues but are considerably compressed along the  $c$  axis owing to the smaller size of lithium compared with sodium atoms. Square-pyramidal  $\text{TiO}_5$  groups are joined in these compounds by tetrahedral  $\text{SiO}_4$  and  $\text{GeO}_4$  groups, respectively.  $^{17}\text{O}$  nuclear magnetic resonance spectra of the two compounds, isotopically enriched with  $^{17}\text{O}$ , showed peaks due to the apical titanyl, Ti—O, and basal, bridging, Ti—O—Si or Ti—O—Ge, oxygen atoms of the title compounds. By comparison with reference spectra, oxygen  $K$  edges and titanium  $L_{2,3}$  edges of electron energy-loss spectra were tentatively assigned.

### 1. Introduction

Titanium occurs in fourfold coordination in a number of compounds, in clearly fivefold coordination in the mineral fersite  $\text{Ba}_2\text{TiOSi}_2\text{O}_7$  and its structural analogues (Masse *et al.*, 1967) but most commonly in octahedral coordination. Distorted octahedral  $\text{TiO}_6$  geometries occur in a number of noncentrosymmetric structure types such as  $\text{LiNbO}_3$ ,  $\text{BaTiO}_3$  and  $\text{KTiOPO}_4$  (KTP) that have important nonlinear optical properties and in centrosymmetric structures such as titanite,  $\text{CaTiOSiO}_4$ .

In the noncentrosymmetric KTP structure, chains of corner-sharing  $\text{TiO}_6$  octahedra are cross linked by phosphate tetrahedra. The short Ti—O titanyl bond leads to essentially fivefold coordination of Ti and is the source of the large nonlinear optical coefficient in KTP. In the centrosymmetric titanite, structure chains of corner-sharing  $\text{TiO}_6$  octahedra are cross linked by sili-

cate tetrahedra (Speer & Gibbs, 1976; Taylor & Brown, 1976). The displacement of the titanium atom from the geometrical centre of the octahedron results in alternating long (1.974 Å) and short (1.766 Å) Ti—O bonds along the chains of octahedra.

A variety of diffraction and spectroscopic techniques has been used to investigate structure-to-property relationships in such materials. These suggest that the local bonding environment of titanium and oxygen atoms plays a key role in their properties. For example, nonlinear optical properties have been correlated with structure in extremely detailed studies by substitution chemistry (*e.g.* Thomas *et al.*, 1990; Phillips *et al.*, 1990).

Other spectroscopic studies include, for example, titanium  $K$ -edge near-edge structure (XANES) measurements of a series of Ti-containing model compounds with different titanium coordination numbers (Farges, 1996). Or again, the chemical shift measured from solid-state Si NMR has been found to vary (Balmer *et al.*, 1997) with the structure and local bonding in a series of titanosilicates.

In the present work, we have chosen to combine diffraction techniques, using X-rays and electrons, to obtain bond lengths and geometry with the spectroscopic techniques of electron energy-loss spectroscopy (EELS) and magic angle spinning (MAS) nuclear magnetic resonance (NMR) to obtain information on energy levels and local environment of the titanium and oxygen atoms that play a key role in the important physical properties of titanosilicates.

The titanosilicate we selected to study was  $\text{Li}_2\text{TiOSiO}_4$ . This material was chosen for several reasons: Firstly, as is shown below, it contains only two oxygen sites in the asymmetric unit of its unit cell, one O atom being a bridging Ti—O—Si and the other an apical O atom of a  $\text{TiO}_5$  tetragonal pyramid. Thus, spectra are simpler to interpret than those of titanite, say, which has four crystallographically inequivalent bridging O atoms or those of KTP which has eight inequivalent bridging O

atoms and two distinct apical O atoms. Secondly, the method of preparation of the title compounds produced well faceted highly perfect crystals that had both reasonable enrichment in the <sup>17</sup>O isotope making them suitable for <sup>17</sup>O NMR study and very low proton content which allows excellent stability in the electron beam used for CBED and EELS. This requirement of low hydrogen content has been emphasized by A. F. Moodie on many occasions. Thirdly, a chemical substitution study was possible as <sup>17</sup>O isotopically enriched crystals of Li<sub>2</sub>TiOGeO<sub>4</sub> could be prepared and these were found to be isostructural with the Si compound.

The ubiquity of oxygen in many important compounds gives <sup>17</sup>O NMR wide-ranging application to solid-state chemistry. For routine observation, <sup>17</sup>O NMR requires isotopic enrichment because of its low natural abundance (0.037%). The large isotropic chemical shift range of <sup>17</sup>O makes it a very sensitive probe of structure and in a wide range of ABO<sub>3</sub> and A<sub>2</sub>BO<sub>3</sub> compounds (*B* = Ti, Zr, Sn) it was shown that the isotropic chemical shift was largely determined by the *B* cation. The multiplicity and extent of splitting of the <sup>17</sup>O resonances are a reflection of the crystal structure (Bastow, Dirken, Smith & Whitfield, 1996). Recently there have been extensive <sup>17</sup>O NMR studies of sol-gel produced oxides, e.g. TiO<sub>2</sub> (Bastow *et al.*, 1993) and HfO<sub>2</sub> (Bastow, Smith & Whitfield, 1996). One of the main advantages of NMR is that it is sensitive to short-range structure so that similar information is obtained from both crystalline and amorphous compounds. In TiO<sub>2</sub>, both OTi<sub>3</sub> and OTi<sub>4</sub> local environments in the amorphous gel and subsequent conversion of anatase to rutile could be followed. Again, in TiO<sub>2</sub>-SiO<sub>2</sub> gel, the formation of Ti-O-Si linkages could be clearly identified (Dirken *et al.*, 1995).

The high resolution that can now be obtained with EELS makes it a powerful technique for probing local environment. Further, the ability to record EELS for both titanium *L*<sub>2,3</sub> edge and oxygen *K* edges makes the technique especially attractive in studying bonding in titanosilicates.

## 2. Experimental

### 2.1. Sample preparation

SiO<sub>2</sub>-TiO<sub>2</sub> mixed gels were prepared by co-hydrolysis by 10 at.% enriched H<sub>2</sub><sup>17</sup>O of an equimolar solution in 2-propanol of titanium *n*-propoxide [Ti(OPr<sup>*n*</sup>)<sub>4</sub>] and tetraethoxyorthosilicate. An equimolar amount of finely powdered lithium carbonate was added to the gel and the mixture stirred for 24 h and then dried under a current of nitrogen to remove ethanol and 2-propanol. The dry powder mixture was heated in a stream of nitrogen to 1170 K for 24 h. The incompletely reacted product was mixed with an equal mass of lithium chloride and reheated to 1170 K in a stream of nitrogen until the lithium chloride had completely evaporated.

The product consisted of a finely crystalline powder which Rietveld analysis of its X-ray powder diffraction pattern showed to consist of Li<sub>2</sub>TiOSiO<sub>4</sub> with 2% admixture of rutile, TiO<sub>2</sub>, and 2% admixture of Li<sub>2</sub>SiO<sub>3</sub>.

Li<sub>2</sub>TiOGeO<sub>4</sub> was prepared by hydrolysis, using <sup>17</sup>O isotopically enriched water, of a stoichiometric mixture of Ti(OPr<sup>*n*</sup>)<sub>4</sub> and Ge(OEt)<sub>4</sub> followed by reaction with an equivalent amount of Li<sub>2</sub>CO<sub>3</sub> at 1170 K. The incompletely reacted product was reheated with an equal mass of LiCl at 1170 K in a stream of nitrogen until the LiCl had completely evaporated. The product consisted of finely crystalline Li<sub>2</sub>TiOGeO<sub>4</sub> with some admixture of rutile and lithium germanate. The preparation of Li<sub>2</sub>TiOGeO<sub>4</sub> has not been reported to our knowledge.

### 2.2. Data collection

X-ray powder diffraction patterns were collected on a Siemens D-500 diffractometer using nickel-filtered Cu *K*α radiation and a graphite monochromator. The powder diffraction patterns were analysed using the Philips Quasar system for Rietveld analysis. This allowed refinement of unit-cell dimensions but not of atom coordinates.

Selected-area and convergent-beam electron diffraction patterns were recorded on an analytical Jeol 2010 electron microscope with an LaB<sub>6</sub> source. Crushed powders were dispersed with absolute ethanol onto holey-carbon-film-covered copper grids and dried in a vacuum oven before insertion into the microscope.

High-resolution electron micrographs (HREM) were recorded on a high-resolution Jeol 4000 EX microscope with an LaB<sub>6</sub> source with a nominal resolution of 1.6 Å.

Electron energy-loss spectra were obtained using a dedicated UHV scanning transmission electron microscope (VG HB501) equipped with a Gatan energy-loss spectrometer (Gatan Imaging Filter model UHV 678). The system uses a cold field-emission source, which allows one to achieve an energy resolution (measured at the full width at half-maximum of the zero-loss peak) of 0.4–0.5 eV.

The MAS NMR experiments were carried out on a Bruker MSL 400 spectrometer (*B*<sub>0</sub> = 9.4 T) operating at 54.2 MHz for <sup>17</sup>O. Oxygen spectra were obtained using a 4 mm double-bearing magic angle probe used with 10–12 kHz spinning speeds, 20 s recycle delay and 1.5 ms pulses (flip angle ~ π/4). Chemical shifts (δ p.p.m.) were measured in parts per 10<sup>6</sup> from an external reference water at a defined shift, δ = 0.

## 3. Results and discussion

X-ray powder diffraction shows crystals of both the title compounds to be tetragonal with unit-cell parameters (refined using the Rietveld analysis program) *a* = 6.4379 (2), *c* = 4.4003 (2) Å for Li<sub>2</sub>TiOSiO<sub>4</sub> and *a* = 6.6110 (8), *c* = 4.4372 (6) Å for Li<sub>2</sub>TiOGeO<sub>4</sub>.

Selected-area and convergent-beam electron diffraction (CBED) of both compounds (Fig. 1) showed that they crystallize in a centrosymmetric tetragonal space group with the only space-group-forbidden reflections being  $hk0$  for  $h+k$  odd. This is consistent with  $P4/nmm$ , the space group confirmed for the corresponding sodium compounds  $\text{Na}_2\text{TiOSiO}_4$  (Nyman *et al.*, 1978) and  $\text{Na}_2\text{TiOGeO}_4$  (Verkhovskij *et al.*, 1970) by successful refinement of their structures from single-crystal X-ray data. This observation, together with the near coincidence of the lattice  $a$  parameters of  $\text{Li}_2\text{TiOSiO}_4$  and  $\text{Na}_2\text{TiOSiO}_4$ , strongly suggested that these compounds are isostructural. The lattice  $c$  parameter of  $\text{Li}_2\text{TiOSiO}_4$  is much less than that of  $\text{Na}_2\text{TiOSiO}_4$  and this is consistent with the two crystals having the same layers of  $\text{SiO}_4$  tetrahedra and  $\text{TiO}_5$  square pyramids joined by sharing corners and separated by layers of  $\text{Li}^+$  ions in the former compound and by the much larger  $\text{Na}^+$  ions in the latter. Fractional atomic coordinates in Table 1 calculated to give the same dimensions of  $\text{SiO}_4$  tetrahedra and  $\text{TiO}_5$  square pyramids were used as a trial structure for calculation of the X-ray powder diffraction pattern. A Rietveld analysis of calculated and observed X-ray powder diffraction intensities gave a Bragg  $R$  value of 0.115 for 42 reflections confirming the trial structure is correct. The  $\text{TiO}_5$  square pyramids have an apical Ti—O bond distance of 1.70 Å and a basal Ti—O bond distance of 1.99 Å.

Crystals of  $\text{Li}_2\text{TiOSiO}_4$  were sufficiently stable in a 400 keV electron beam to obtain high-resolution electron micrographs (Fig. 2). These verify that the crystals have large regions of single phase without extended defects.

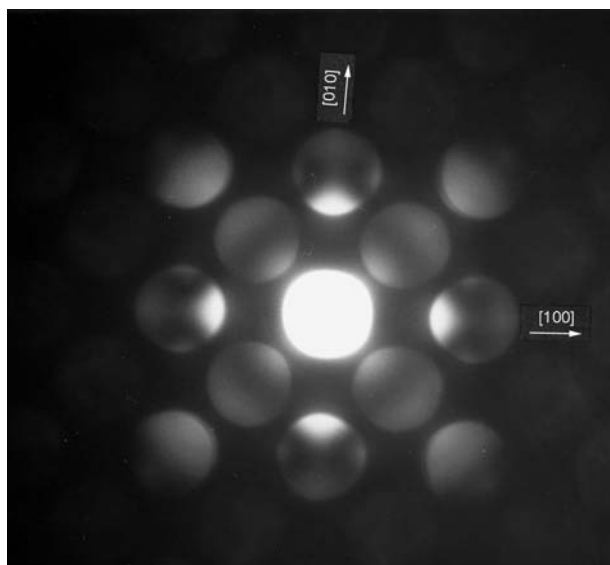


Fig. 1. CBED of  $\text{Li}_2\text{TiOSiO}_4$  viewed along  $[001]$ , showing systematic absences  $hk0$  for  $h+k \neq 2n$ .

Table 1. Fractional atomic coordinates of  $\text{Li}_2\text{TiOSiO}_4$

		$x$	$y$	$z$	$B$ (Å <sup>2</sup> )
Ti	2(c)	1/4	1/4	0.076	0.5
Li	4(e)	0	0	1/2	0.5
Si	2(a)	3/4	3/4	0	0.5
O(1)	8(i)	1/4	0.957	0.213	0.5
O(2)	2(c)	1/4	1/4	0.700	0.5

The  $^{17}\text{O}$  MAS NMR spectra reveal details of the solid-state formation of  $\text{Li}_2\text{TiOSiO}_4$  via an amorphous gel to a final crystalline product. The spectrum (Fig. 3, bottom) of the reaction mixture heated to 970 K is characteristic of an amorphous gel. There are two main resonances, one at  $\sim 0$  parts in  $10^6$  and the other at  $\sim 180$  parts in  $10^6$ . By comparison with NMR data from  $\text{TiO}_2$ - $\text{SiO}_2$  gels (Dirken *et al.*, 1995), these can be assigned to Si—O—Si at 0 parts in  $10^6$  and Si—O—Ti at 180 parts in  $10^6$ . There is also a minor peak at  $\sim 540$  parts in  $10^6$ , which is probably  $\text{OTi}_3$ . The amorphous nature, which was confirmed by XRD, is indicated by the line widths of the resonances associated with titanium. After heating to 1170 K, crystallization has clearly occurred from the much reduced line widths (Fig. 3, centre). Four peaks can be immediately identified at  $\sim 40$ , 372, 406 and 595 parts in  $10^6$ . From the  $^{17}\text{O}$  NMR shift data that already exist, the peak at 595 parts in  $10^6$  can be immediately identified as rutile (Bastow *et al.*, 1993) and the peaks at 372 and 406 parts in  $10^6$  as  $\text{Li}_2\text{TiO}_3$ . The resonance at  $\sim 40$  parts in  $10^6$  has second-order quadrupolar structure and the decrease in width from the Si—O—Si linkage is indicative of a nonbridging silicate unit, and given the stoichiometry is probably a lithium silicate. XRD indicated that  $\text{Li}_2\text{SiO}_3$  is present. This information could be gleaned directly from O MAS NMR if a sufficiently large database of  $^{17}\text{O}$  spectra from crystalline compounds existed.

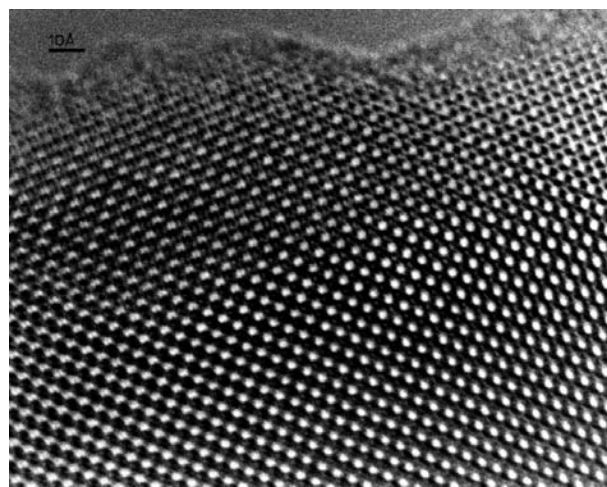


Fig. 2. High-resolution electron micrograph of  $\text{Li}_2\text{TiOSiO}_4$  viewed along  $[001]$ .

On heating to 1220 K, the <sup>17</sup>O MAS NMR spectrum becomes more complex (Fig. 3, top). The rutile and lithium silicate peaks have decreased in intensity whereas that from the Li<sub>2</sub>TiO<sub>3</sub> has increased. There are new peaks, a prominent one at around 150 parts in 10<sup>6</sup> and a second at 730 parts in 10<sup>6</sup>, which must be the oxygen resonances from Li<sub>2</sub>TiOSiO<sub>4</sub>. Recrystallization from an LiCl melt produced almost single-phase Li<sub>2</sub>TiOSiO<sub>4</sub> (Fig. 4). There are two distinct oxygen sites in Li<sub>2</sub>TiOSiO<sub>4</sub> in the ratio 4:1. The more populated from the Si—O—Ti linkages give rise to the peak at ~150 parts in 10<sup>6</sup>. An experiment at 7.05 T showed that the width scaled inversely with the applied magnetic field as expected for a purely second-order quadrupolar broadened line shape. This was simulated to give a quadrupole constant,  $C_q$ , of 3.05 MHz, asymmetry parameter of 0.35 and an isotropic chemical shift of 157.0 parts in 10<sup>6</sup>. These shift data are extremely useful in confirming the assignment of resonances in this region from TiO<sub>2</sub>—SiO<sub>2</sub> gels. The other resonance has a very high shift at 741 parts in 10<sup>6</sup>. In coordination with titanium, <sup>17</sup>O can show a wide range of chemical shifts, depending strongly on the coordination number of the

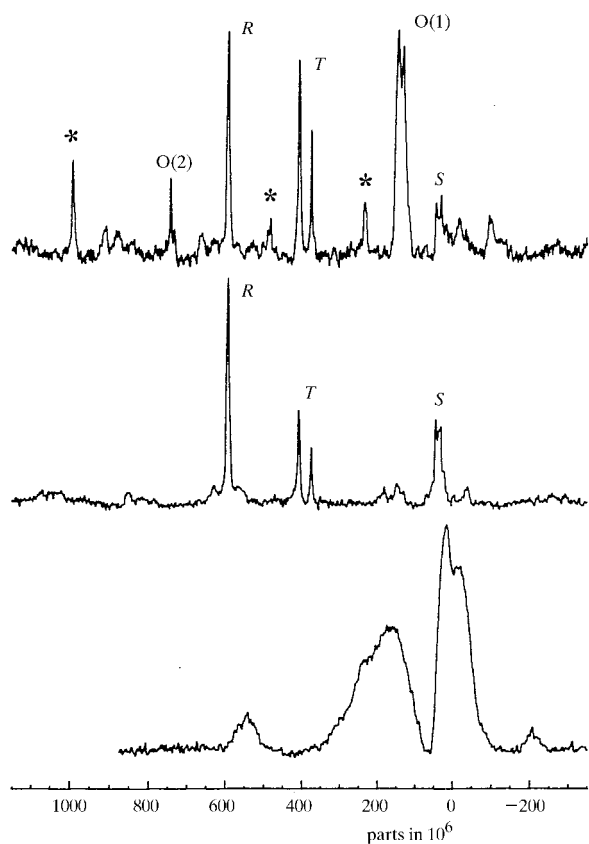


Fig. 3. <sup>17</sup>O MAS NMR of TiO<sub>2</sub>/SiO<sub>2</sub>/Li<sub>2</sub>CO<sub>3</sub> reacted at 970 K (bottom), 1170 K (middle) and 1230 K (top). O(1), O(2) indicate resonances from Li<sub>2</sub>TiOSiO<sub>4</sub>, T from Li<sub>2</sub>TiO<sub>3</sub>, S from Li<sub>2</sub>SiO<sub>3</sub>, R from rutile and asterisks indicate side bands from the O(2) resonance.

oxygen. At 741 parts in 10<sup>6</sup>, this can be assigned to the nonbridging apical oxygen of the TiO<sub>5</sub> tetragonal pyramid. The highly linear nature of the local environment is reflected in the strong chemical-shift anisotropy, which gives rise to the extensive spinning sideband pattern from this site. The centre band, which is not the strongest peak, is identified from several long runs at different spinning frequencies.

The MAS NMR spectrum of <sup>17</sup>O from Li<sub>2</sub>TiOGeO<sub>4</sub> (Fig. 4) is similar to that from the silicate, and the resonances from the apical and basal oxygens of the TiO<sub>5</sub> tetragonal pyramids can be unequivocally assigned. The resonance from the apical nonbridging atom occurs at 749 parts in 10<sup>6</sup> (cf. 741 parts in 10<sup>6</sup> for the silicate). The resonance at around 105 parts in 10<sup>6</sup> from the bridging Ti—O—Ge oxygen has characteristic second-order quadrupolar line shape with peaks at 82 and 128 parts in 10<sup>6</sup> (cf. 131 and 145 parts in 10<sup>6</sup> for the silicate). The bigger splitting of this peak in the germanate compared with the silicate is a reflection of the bigger  $C_q$  in the germanate. A simulation of the quadrupole broadened line shape for this resonance gave a quadrupole coupling constant of 4.80 MHz, asymmetry parameter of 0.22 and an isotropic chemical shift of 148 parts in 10<sup>6</sup>. An excellent agreement between observed and simulated line shapes reflects the fact there is only one bridging oxygen site in the asymmetric unit of the unit cell.

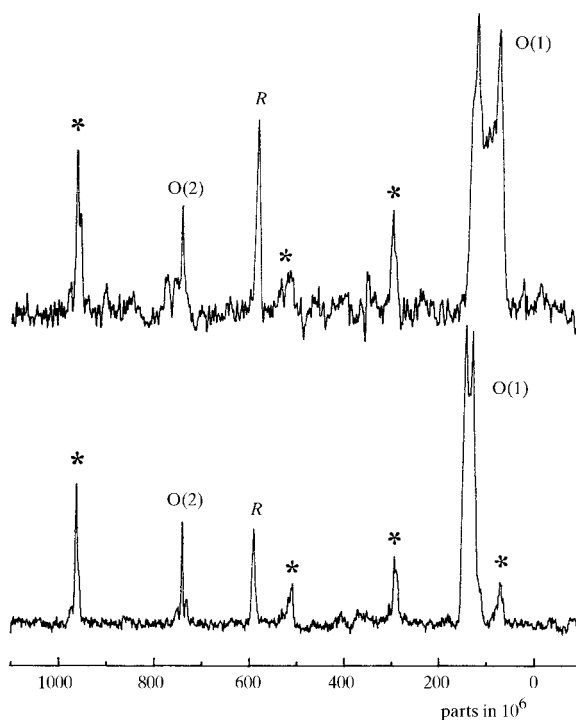


Fig. 4. <sup>17</sup>O MAS NMR of Li<sub>2</sub>TiOSiO<sub>4</sub> (lower curve) and Li<sub>2</sub>TiOGeO<sub>4</sub> (upper curve). Resonances from apical O(2) and bridging O(1) sites are indicated; R indicates resonance from rutile; spinning side bands from the O(2) resonances are indicated by asterisks.

The oxygen  $K$  edges in the EELS spectra of  $\text{Li}_2\text{TiOSiO}_4$  and  $\text{Li}_2\text{TiOGeO}_4$  show that there are mainly four peaks near the edge threshold and the energy of these changes significantly when comparing the two compounds (Fig. 5). These edges arise from transitions from the oxygen  $1s$  core states to unoccupied states having  $p$  symmetry and probe the local electronic structure at the oxygen sites (therefore the  $O-p$  states). It is difficult to unambiguously associate the peak positions with particular energy bands without detailed molecular-orbital or band-structure methods but from reference spectra in the  $\text{Ti-O}$  and  $\text{Si-O}$  systems a general description of the peaks can be given.

In  $\text{SrTiO}_3$ , anatase, and rutile, the first peak of the  $O$   $K$  edge is at about 530 eV (e.g. van der Laan, 1990) and it represents the hybridization of the  $O-2p$  band with the  $\text{Ti-}3d$  bands. In these reference materials and in titanite ( $\text{CaTiSiO}_5$ ), the degeneracy of the  $3d$  states is lifted due to the octahedral crystal field (even if distorted) and thus these states are split into  $t_{2g}$  and  $e_g$  bands which are clearly visible in the  $\text{Ti } L_{2,3}$  edges of these compounds (e.g. Brydson *et al.*, 1992). In  $\text{Li}_2\text{TiOSiO}_4$  and  $\text{Li}_2\text{TiOGeO}_4$ , the  $\text{Ti } L_{2,3}$  edge (Fig. 6) does not show such even splitting between the two states owing to the lower symmetry of the square-pyramidal coordination of  $\text{Ti}$  and from this it can be deduced that such splitting ( $t_{2g}$  and  $e_g$ ) should not be visible in the  $O$   $K$  edge. The structure at about 535–536 eV is very similar in shape and position to the peak seen when oxygen is coordinating  $\text{Si}$  tetrahedrally [see for example the spectra of Wallis & Gaskell (1993)] and the peak arises from the mixing of the  $\text{Si-}3s/3p$  states with the  $O-2p$ . The similarity in energy positions of the  $\text{Ti-O}(1)$  and  $\text{Si-O}(1)$  peaks arises in part because of the comparable bond lengths in the reference materials and in our compounds. In fact, the  $\text{Si-O}$  bond length in the  $\text{Si}$  tetrahedra of  $\text{Li}_2\text{TiOSiO}_4$  and in  $\alpha\text{-SiO}_2$  are very similar ( $\sim 1.6$  Å) and the  $\text{Ti-O}(1)$  bridging bonds in  $\text{Li}_2\text{TiOSiO}_4$  and anatase (or rutile) are also very similar ( $\sim 1.9$  Å). Considering these similarities to spectra of  $\text{Ti-O}$  and  $\text{Si-O}$  compounds, we can see that the  $O$   $K$  edges show the

mixed bonding character when forming the  $\text{Ti-O-Si}$  bridges bonding with the  $\text{Ti } 3d$  bands and the  $\text{Si } 3s/sp$  bands at different energy levels.

From the shorter bond length  $\text{Ti-O}(2)$  of the apical oxygen (1.70 Å), it can be deduced that the peak position should be at higher energy than the 529 eV peak arising from  $\text{Ti-O}(1)$ . The peak at 532–533 eV can therefore be assigned to the formation of this bond between the  $\text{Ti-}3d$  and the apical  $O-2p$ . Although detailed calculations are necessary to confirm the exact origin, the structure at about 540 eV can be tentatively assigned to more delocalized states mixing both together the  $\text{Ti-}4s/4p$  and the  $\text{Si-}3s/sp$  with the  $O-2p$  as similar structures are generally observed in transition-metal oxides and not in any of the  $\text{Si-O}$  reference materials.

We note that remarkable peak shifts are observed when comparing  $\text{Li}_2\text{TiOSiO}_4$  and  $\text{Li}_2\text{TiOGeO}_4$  spectra reflecting the change in bond distances. In particular, we note the separation between the high-energy peaks related to  $\text{Si}$  (and  $\text{Ge}$ ) increases in the same way as the quadrupole coupling constant calculated from the NMR of the bridging  $O$  atoms.

#### 4. Conclusions

Lithium titanium silicate,  $\text{Li}_2\text{TiOSiO}_4$ , and lithium titanium germanate,  $\text{Li}_2\text{TiOGeO}_4$ , were shown by selected-area and convergent-beam electron diffraction to have the space group  $P4/nmm$ . X-ray powder diffraction patterns were indexed and accurate cell dimensions for the two compounds determined. An excellent fit of calculated and observed X-ray powder diffraction was achieved.

$^{17}\text{O}$  nuclear magnetic resonance spectra of the two compounds, isotopically enriched with  $^{17}\text{O}$ , showed peaks due to the apical titanyl,  $\text{Ti-O}$ , and basal bridging  $\text{Ti-O-Si}$  or  $\text{Ti-O-Ge}$  oxygen atoms of the title compounds. By comparison with reference spectra, oxygen  $K$  edges and titanium  $L_{2,3}$  edges of electron energy-loss spectra were tentatively assigned.

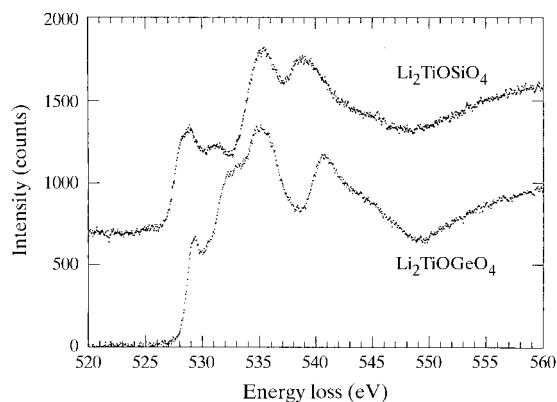


Fig. 5. EELS  $O$   $K$  edge of  $\text{Li}_2\text{TiOSiO}_4$  and  $\text{Li}_2\text{TiOGeO}_4$ .

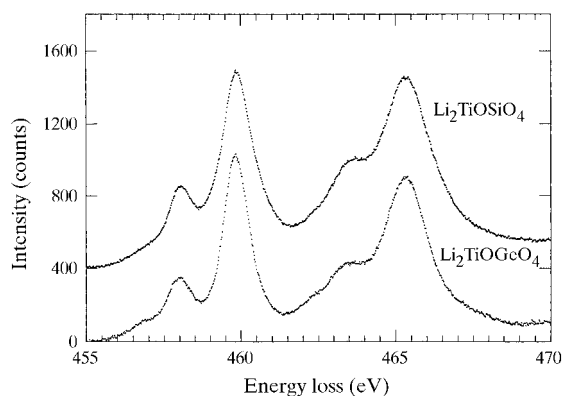


Fig. 6. EELS  $\text{Ti } L_{2,3}$  edge of  $\text{Li}_2\text{TiOSiO}_4$  and  $\text{Li}_2\text{TiOGeO}_4$ .

We plan to extend this work to <sup>17</sup>O NMR and oxygen K-edge and titanium L<sub>2,3</sub>-edge EELS of more complex titanosilicates and of related titanophosphates and to make detailed calculations that will allow us to unambiguously associate the EELS peak positions to particular energy bands.

MES thanks EPSRC for funding <sup>17</sup>O NMR research through GR/L28647.

### References

- Balmer, M. L., Bunker, B. C., Wang, L. Q., Peden, C. H. F. & Su, Y. (1997). *J. Phys. Chem.* **B101**, 9170–9179.
- Bastow, T. J., Dirken, P. J., Smith, M. E. & Whitfield, H. J. (1996). *J. Phys. Chem.* **100**, 18539–18545.
- Bastow, T. J., Moodie, A. F., Smith, M. E. & Whitfield, H. J. (1993). *J. Mater. Chem.* **3**, 697–702.
- Bastow, T. J., Smith, M. E. & Whitfield, H. J. (1996). *J. Mater. Chem.* **6**, 1951–1955.
- Brydson, R., Sauer, H. & Engel, W. (1992). *Transmission Electron Energy Loss Spectrometry in Materials Science*, edited by M. M. Disko, C. C. Ahn & B. Fultz, pp. 131–154. Warrendale, PA: The Minerals, Metals and Materials Society.
- Dirken, P. J., Smith, M. E. & Whitfield, H. J. (1995). *J. Phys. Chem.* **99**, 395–401.
- Farges, F. (1996). *J. Non-Cryst. Solids*, **204**, 53–64.
- Laan, G. van der (1990). *Phys. Rev. B*, **41**, 12366–12368.
- Masse, R., Grenier, J.-C. & Durif, A. (1967). *Bull. Soc. Fr. Minéral. Cristallogr.* **90**, 20–23.
- Nyman, H., O'Keefe, M. & Bovin, J.-O. (1978). *Acta Cryst.* **B34**, 905–906.
- Phillips, M. L. F., Harrison, W. T. A., Gier, T. E., Stucky, G. D., Kulkarni, G. V. & Burdett, J. K. (1990). *Inorg. Chem.* **29**, 2158–2163.
- Speer, J. A. & Gibbs, G. V. (1976). *Am. Mineral.* **61**, 238–247.
- Taylor, M. & Brown, G. E. (1976). *Am. Mineral.* **61**, 435–447.
- Thomas, P. A., Glazer, A. M. & Watts, B. E. (1990). *Acta Cryst.* **B46**, 333–343.
- Verkhovskij, V. J., Kuz'min, E. A., Iljukhin, V. V. & Belov, N. V. (1970). *Dokl. Akad. Nauk SSSR*, **190**, 91–93.
- Wallis, D. J. & Gaskell, P. H. (1993). *Electron Microscopy and Analysis*, edited by A. J. Craven, pp. 47–50. Institute of Physics Conference Series No. 138. Bristol: Institute of Physics.